


Article

# Study on Surface Properties of Polyamide 66 Using Atmospheric Glow-Like Discharge Plasma Treatment

Mingyang Peng <sup>1</sup> , Lee Li <sup>1,\*</sup>, Jiaming Xiong <sup>1</sup>, Kui Hua <sup>1</sup>, Shufan Wang <sup>1</sup> and Tao Shao <sup>2</sup>

<sup>1</sup> State Key Laboratory of Advanced Electromagnetic Engineering and Technology, School of Electrical and Electronic Engineering, Huazhong University of Science and Technology (HUST), Wuhan 430074, China; pengmingyang@hust.edu.cn (M.P.); xjm@hust.edu.cn (J.X.); M201671453@hust.edu.cn (K.H.); U201411827@hust.edu.cn (S.W.)

<sup>2</sup> Institute of Electrical Engineering, Chinese Academy of Sciences, Beijing 100190, China; st@iee.ac.cn

\* Correspondence: leeli@hust.edu.cn; Tel./Fax: +86-27-8755-9349

Received: 27 May 2017; Accepted: 9 August 2017; Published: 14 August 2017

**Abstract:** Surface modification of fiber fabric sometimes needs a large volume of cold plasma to improve its efficiency. This experimental study is based on the treatment of polyamide 66 (PA66) fabrics using large contact-area glow-like plasma, which are produced in the atmospheric air without any dielectric barriers. The atomic force microscopy (AFM) and X-ray photoelectron spectroscopy (XPS) are adopted, respectively, to detect the surface changes in physical microstructure and the variations in the type and quantity of chemical functional groups. The results show that the PA66 fabric surface will be etched remarkably by the glow-like plasma, and the surface roughness and the surface energy are augmented. On the surface of the processed PA66 fabrics, the oxygen-containing functional groups' content rises together with the decrease on the total primary C–C and C–N bonds. After 30 seconds of sterilization by the glow-like plasmas, most of the bacterial colonies on the fabric vanish. The effectiveness of this kind of plasma treatment could last for three days in a sealed environment.

**Keywords:** atmospheric pressure; glow-like discharge; polyamide 66 (PA66); surface modification; sterilization; aging effect

## 1. Introduction

Making use of cold plasma on the surface modification in organic polymer materials has become a new technique. Compared with other methods in material surface modification, this new technique is a relatively environmentally friendly drying and processing method, reducing the use of chemical reagent and water. In addition, the treatment on the material surface mainly depends on the collisions between the processing materials and high-energy electrons, excited or metastable particles in the plasmas. The material surface is modified for tens of nanometers, and without an obvious effect on their physical structures and internal characters [1–4].

The treatment effect achieved by the cold plasma reflects on both physical and chemical aspects. The experimental results of Nakahira et al. showed that, through a short time treatment, the cold plasma could change the roughness of the organic glass surface at a relatively low power, and the superficial area of the material would increase [5]. Zhang, Shao et al. [6] applied atmospheric pressure argon plasma jets, to modify the polymethyl-methacrylate. According to their report, after the plasma jet treatment, the surface flashover performance of polymethyl-methacrylate is effectively improved. Meiners et al. researched the influences on the hydrophilicity of polypropylene films processed by atmospheric air plasma, which were generated by DBD (dielectric barrier discharge) [7]. The results showed that the hydrophilicity of the processed polypropylene films improved. With further measurement, the surface tension of the processed polypropylene films increased by 72 mN/m.

Yuri et al. studied on the surface chemical influences of nonthermal plasmas on the PE (polyethylene), PP (polypropylene), PET (polyethylene terephthalate) and polyester fabrics [8,9]. It was shown that the polyester material gained a better hydrophilicity in a short time with the generation of new function groups. According to the research of Lai et al. [10] they founded that C=O, C–O, COOH and C–NH<sub>2</sub> appeared on the polymer film under the plasma process. Furthermore, the carbonyl group was an important factor to improve the hydrophilicity; the contact angle decreased with the increase of the carbonyl.

Up to now, most of the surface modification studies are focused on plasma jet or dielectric barrier discharge (DBD) and atmospheric air. However, for plasma jet, the jet array is needed to obtain larger treatment area. But the dark area will exist between the jet tubes—other means like moving the unprocessed sample is taken for its application. As for DBD, the dielectric barriers will cause plasma pollution. Meanwhile, the discharge size is limited in the direction of the discharge. According to recent studies, integrating wire electrodes with repetitive nanosecond pulses had become an effective method to generate large-volume stable, glow-like diffuse plasmas in atmospheric pressure air without a dielectric barrier [11,12], which is a kind of uniform plasma, attracting much attention [13,14].

Accordingly, this paper has designed a surface modification reactor using a cylindrical discharge chamber, which can generate cylindrical cold plasmas in an air environment without any dielectric barriers. To verify the potency of this kind of plasma in material modification, especially the high molecular polymer, we chose nylon fabric to be the test object. The X-ray photoelectron spectroscopy (XPS) and atomic force microscopy (AFM) were adopted to investigate the nylon surface changes in terms of physical microstructure and the variations in the type and quantity of polar functional groups, both before and after the plasma treatment. For the widespread application of the high molecular polymer, such as in the textile and medical industries [15,16], the surface modification and the sterilizing effect of the processed nylon material under different discharge conditions are observed. Also, the timeliness of this kind of plasma treatment is studied. The research results of this paper may provide a new idea for the surface modification of polymer materials.

## 2. Experimental Section

### 2.1. Nylon Materials

The nylon material used in this study is a kind of polyamide 66 (PA66) fiber fabric. The mesh number of the treated PA66 fabrics is 400 (38 μm pore size). Generally, PA66 fabric has poor hydrophilicity, the surface-to-volume ratio is low, and it is hard to color [17]. Previously, chemical processing was usually employed in the surface modification of the PA66 fabric. But the process was complex, the cost was high, the polluted water produced during the process did harm to the environment [1,18]. On the other hand, in terms of medical application, the material needed to be sterilized, the traditional methods liked pasteurization was cumbersome, and it wasted a good deal of time and energy. Figure 1 gives the microstructure of the PA66 fabric observed by scanning electron microscope. Before the plasma processing, the alcohol and deionized water are used to sterilize and clean up the samples, and then drying for 1 h in a vacuum drying device.

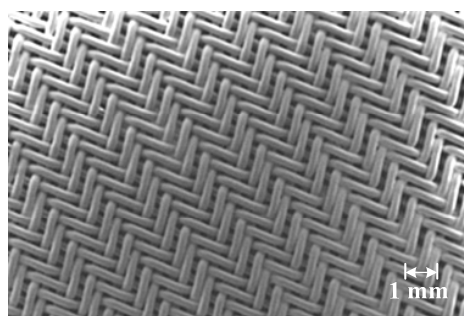


**Figure 1.** Microstructure of the PA66 fabric observed by scanning electron microscope.

## 2.2. Surface Modification Reactor

The whole surface modification reactor consists of a repetitive nanosecond pulse generator, which is designed and made by our laboratory, and a cylinder reactor. As is shown in the dash box of Figure 2, the nanosecond pulse generator is mainly composed of a repetitive charging circuit, a Tesla transformer and a sharpening switch. The repetitive charging circuit is formed by a DC supply, a storage capacitor  $C_{main}$  (2 mF), a charging thyristor  $S_{ch}$  and a charging inductor  $L_{ch}$ . The output voltage of the DC supply is adjustable. After  $S_{ch}$  turns on,  $C_1$  (10  $\mu$ F) will be resonantly charged by  $C_{main}$  through  $L_{ch}$ .

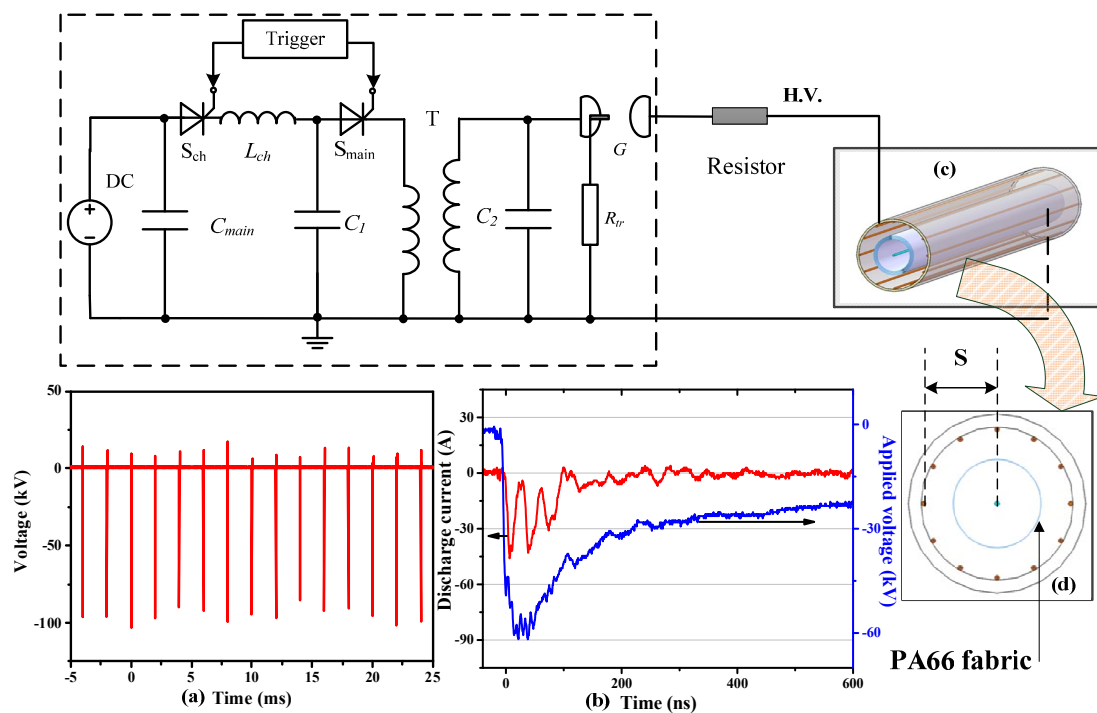


**Figure 2.** Schematic diagram of the reactor: (a) The output pulse voltage waveform; (b) The typical voltage and current waveforms; (c) The 3D view (the orange electrodes are the high-voltage terminals and the blue one is the ground pole. The blue barrels represent the fabrics waiting to be processed); (d) Side view of the position of the PA66 fabrics to be treated.

After being charged to a defined voltage,  $C_1$  discharges through a controllable, fast thyristor  $S_{main}$ . Afterwards, high voltage will be obtained across the secondary ceramic capacitor  $C_2$  (0.1 nF) of the Tesla transformer  $T$ . A trigatron gap is selected as sharpening switch  $G$ . After being sharpened by a sharpening switch  $G$ , repetition nanosecond pulses will be obtained.  $G$  is designed to break down at nearly the maximum voltage across  $C_2$ . The trigger electrode of  $G$  is connected to the ground through a resistor  $R_{tr}$  of 1.0 M $\Omega$ . Controlled by the trigger at repetition frequency, the primary capacitor  $C_1$  (10  $\mu$ F) is alternant in the state of charge/discharge through a charging thyristor  $S_{ch}$  and a controllable fast thyristor  $S_{main}$ . The output pulse voltage and current waveforms are shown in Figure 2a,b. The maximum peak voltage is 100 kV, the rise-time is around 25 ns every pulse, the full width at half maximum (FWHM) is  $\sim$ 750 ns. The pulse repetition frequency (PRF) can vary from 1 to 500 Hz.

The discharge chamber adopts a multirod-to-cylinder electrode configuration. The 3D image of the cylindrical electrode configuration is given by Figure 2c, the high-voltage (H.V.) terminals and ground pole are marked in different colors (orange and blue). Additionally, for the purpose of the uniformity and the larger volume of glow-like plasmas [19], the number of high-voltage poles surrounding the grounding pole is set as 12, making the distance between the ground and high-voltage terminal to be 4.0 cm. The material of these poles is straight, bare copper wires. The diameter of the chosen copper wires is 2.0 mm, and the length is 50.0 cm. All the electrodes are parallel to each other.

Figure 2d gives the side image of the cylindrical electrode configuration. The mutual alignment of the high-voltage terminal, the PA66 fabrics and the ground pole can be fixed by some independent insulation-supporting structure. Meanwhile, the discharge chamber can be rotated in certain speed, which can lead to uniform treatment efficiency.

The whole process is performed in atmospheric air. Figure 3a shows the main view of the cylindrical electrode configuration in discharge and Figure 3b gives the side view of the discharge with one pair of electrodes; the PRF is set as 500 Hz. Figure 3c gives the photo of PA66 fabric being treated. Based on previous studies [19], the plasma temperature is about 300 K. As shown in Figure 2b, the first current peak is mainly composed of the displacement current and the following oscillation is the conduction current superimposed on the displacement current with opposite polarity. The current amplitude in Figure 2b has been up to dozens of amperes and much greater than those of known typical corona and glow discharge under low pressure. This kind of discharge is diffuse, having the evident characteristics of glow discharge, which demonstrates the particularity of this air's glow-like plasma. From the Figure 3a, we can see that the atmospheric-air glow-like plasma fill up the entire discharge chamber; there is no apparent dark space. The plasma channels develop between all of the H.V. and grounding poles. By employing longer wire electrodes with the corresponding matching circuit, it is possible to obtain a larger volume of glow-like plasmas.



**Figure 3.** Images of the glow-like discharge: (a) The main view of the cylindrical electrode configuration in discharge; (b) The side view of the discharge with one pair of electrodes; (c) The PA66 fabric being treated.

### 2.3. Measurement Instruments

The atomic force microscope (AFM) is the Japanese Shimadzu model SPM9700 (Shimadzu, Kyoto, Japan), which is applied to detect the changes of the surface microcosmic three-dimensional (3D) structure under different glow-like discharge condition, before and after the treatment. This AFM instrument can do 3D scanning of the nylon fabric surface. The lateral resolution is 2.0 nm. This microscope has two microcantilevers, which are very sensitive to the weak force. When one microcantilever is settled, the other installs a tiny probe. During the test, the tiny probe touches the sample surface, and scans the area. The tip atom of the tiny probe has weak repulsive force against the sample surface; the microcantilever with its tiny probe moves on the surface in waves. It can obtain the equipotential surface of the atomic force between the tip atom and the sample surface, and then it can get the morphology information of the sample surface.

The X-ray photoelectron spectroscopy (XPS) is used to analyze the surface of the processed PA66 fabrics. The instrument is the Japanese Shimadzu-Kratos model AXIS-ULTRA DLD-600 W X-ray photoelectron spectrometer (Shimadzu-Kratos, Manchester, UK). The source is the Bi-anode Al/Mg X-ray source, the spatial resolution is less than 3  $\mu\text{m}$ , the acceptance angle is 90°, and the vacuum degree is  $10^{-7}$ – $10^{-8}$  Pa. The corresponding reference signal is the C1s signal with a binding energy of about 285 eV. XPSpeak software (Version 4.1, Dr. Raymond Kwok, Hong Kong, China) is used to analyze the data. The fitting method is the Gaussian–Lorentzian curves while wiping off the Shirley background.

### 3. Results and Discussion

#### 3.1. Physical Analysis of the Surface

The AFM is adopted to scan the control group. Samples are processed at 10 and 60 s, while the peak voltage is about 90 kV and the PRF is set as 500 Hz. The scanning area is  $1 \mu\text{m} \times 1 \mu\text{m}$ , and Figure 4 shows the scan results.

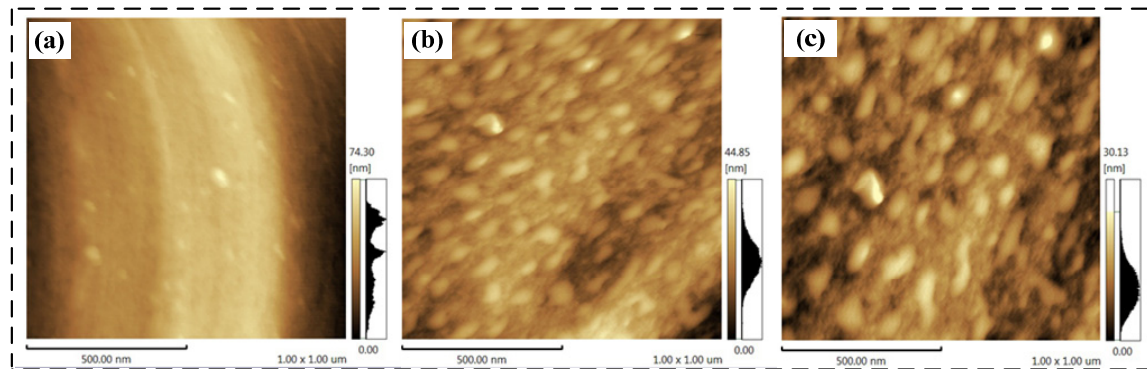


**Figure 4.** AFM photos of the samples under different treatment conditions: (a) Control; (b) Processed for 10 s; (c) Processed for 60 s.

As is shown in Figure 4a, the unprocessed sample surface seems to be very flat. It has few protrusions. The surface roughness ( $R_a$ ) of the control sample is 3.794 nm. Through Figure 4b,c, after the glow-like plasma treatment, many protrusions have appeared on the fabric surface. Moreover, the  $R_a$  increases to 7.221 and 8.392 nm, respectively. The surface becomes rougher with the increase of the processing time. Nevertheless, the augment of the protrusion number from 10 to 60 s is not significant. It indicates that the surface of the PA66 fabric is modified, and there isn't an obvious effect on its internal characteristics. As an important feature, the amelioration of the fabric's hydrophilic characteristic can be recognized by this etching phenomenon [20,21]. The plasma etching can cause the surface to become rough with the crosslinking on the surface and incorporation of polar functional groups, which leads to the cracking of macromolecules and the degrading of the surface layer. Accordingly, the hydrophilicity of the PA66 material can be improved.

As is shown in Figure 1, there are some micron-sized apertures between the filaments that constitute the PA66 fabric. The plasmas will traverse these apertures, which are acting as the channels. This demonstrates that after the stable or metastable state, active particles, including high-energy electrons, arrive at the surface of the PA66 fabric. A few of these act on the fabric surface. However, most of the particles will go through the fibrage. There will be several collisions, but under the effect of the electric field, they will continue to accelerate and ionize the air in the gap until reaching the ground.

On the other hand, the protrusions on the fabric obtained by the glow-like plasma process are distributed relatively evenly. As such, the corresponding treatment's efficiency is proved to be homogeneous by this phenomenon.

#### 3.2. Chemical Analysis of the Surface

Figure 5 shows the spectra characteristics of the PA66 fabrics, unprocessed and processed, with different treatment times, while the peak voltage is about 90 kV and the PRF is set as 500 Hz.

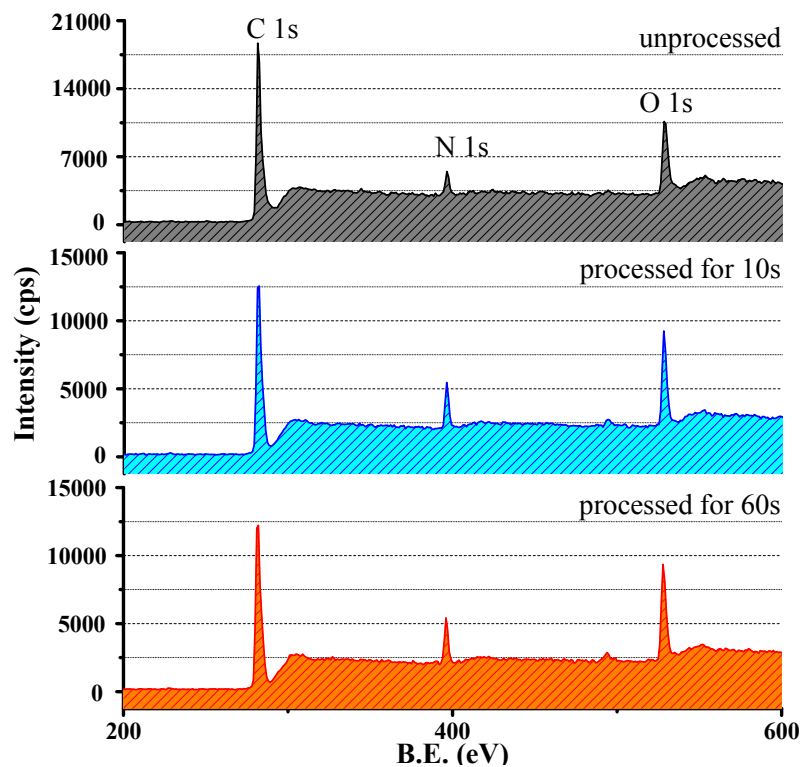


**Figure 5.** X-ray photoelectron spectroscopy (XPS) scan of unprocessed PA66 fabric and the glow-like plasma processed samples.

Table 1 and Figure 6 give the details about the relative chemical compositions and atomic ratios for the PA66 fabric unprocessed and processed by glow-like plasma obtained by XPS. The element content is calculated by the ratio of the corresponding integral area of the peaks. As shown in the XPS spectrums in Figure 5, it is obvious that the highest C1s peak occurs on the control group. After the plasma treatment, the C-element content of the processed sample reduces significantly. Meanwhile, O-element content is augmented distinctly. N-element content has also changed. Some polar functional groups will be imported into the nylon material surface by the glow-like plasma processing [22,23], which results in the microstructural changes of the fiber surface. In addition, the relevant chemical bonds are cracked and the new functional groups are generated—all of these will be represented by the C-, O- and N-element content changes of the XPS spectrums. With the increase of the treatment time, the element's content-varying amplitude will become more notable.

To make further analyses about the changes on the types and ratios of the surface functional groups, the C1s and O1s spectra are analyzed by XPS peak. As is shown in Figure 6, the C1s peak of unprocessed fabrics is able to be divided into four peaks, they respectively indicate four carbon-containing groups: C–C (285.0 eV), C–N (285.3 eV), C–O/C–OH (286.5 eV) and CONH (288.0 eV) [24,25]. Table 2 gives the relative amounts of carbon-containing groups for various peaks, and then Figure 6 gives the peak splitting diagrams of the samples processed at 10 s and 60 s; the corresponding changes of the contents of carbon functional groups are shown in Table 2, line 2&3.

The O1s XPS spectra under different conditions are shown in Figure 7. The O1s peak of the fabrics is able to be divided into two peaks; they indicate two oxygen-containing groups: C–O/C–OH (533.3 eV), CONH/COOH (531.6 eV) [26,27]. Table 3 gives the relative content of oxygen-containing groups corresponding to each peak. It is shown that, when the treatment time is 10 s, the ratio of C–O/C–OH increases from 10.04% to 18.06%, and the content of CONH/COOH decreases from 89.96% to 81.94%. When the treatment time reaches 60 s, the content of C–O/C–OH increases from 10.04% to 47.10%; the content of CONH/COOH decreases from 89.96% to 52.90%.

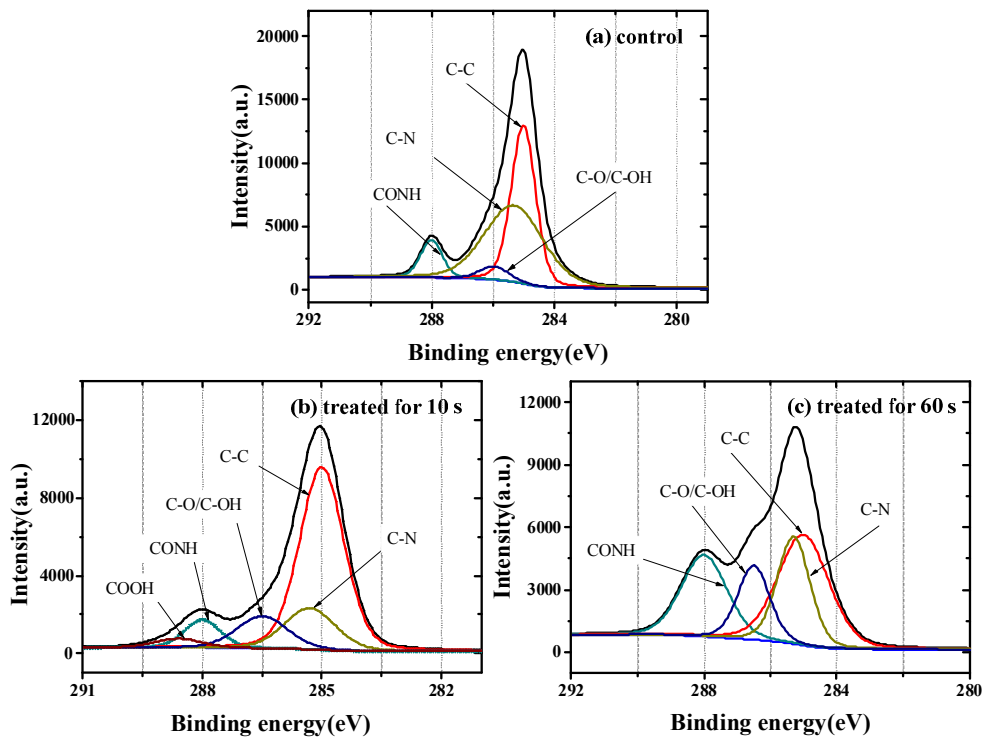


**Figure 6.** Synthesis curve of C1s-spectrums of the control and glow-like plasma processed samples. (a) Control; (b) Treated for 10 s; (c) Treated for 60 s.

**Table 1.** Relative element contents and atomic ratios.

Sample	Element Content (%)				Ratio	
	C1s	O1s	N1s	O/C	N/C	(O + N)/C
Control	77.93	13.75	8.32	0.18	0.11	0.29
Processed 10 s	76.63	16.38	6.99	0.21	0.10	0.31
Processed 60 s	72.40	18.76	8.84	0.26	0.12	0.38

**Table 2.** Corresponding contents of various carbon-containing groups (%).

Sample	Carbon-Containing Groups (%)				
	C–C	C–N	C–O/C–OH	CONH	COOH
Control	40.35	47.05	4.06	8.54	0
Processed 10 s	60.87	15.87	12.36	7.59	3.30
Processed 60 s	37.00	23.05	15.54	24.42	0

**Table 3.** Corresponding contents of various oxygen-containing groups (%).

Sample	Oxygen-Containing Groups (%)	
	C–O/C–OH	CONH/COOH
Control	10.04	89.96
Processed 10 s	18.06	81.94
Processed 60 s	47.10	52.90

It is shown that the total amount of C–C bonds and C–N bonds on the unprocessed sample, the processed 10 s sample and the processed 60 s sample are 87.4%, 76.74% and 60.05%, respectively. The oxygen-containing groups' content rises together with the decrease of the primary C–C and C–N

bonds in all. The primary carbon-containing bonds are cracked by the glow-like plasmas, which is helpful to generate hydroxyl, carboxyl and double bonds of carbon to oxygen under atmospheric air conditions. Furthermore, these hydrophilous groups are beneficial to the enhancement of the samples' hydrophilicity. The CONH is the primary chemical bond in the polyamides molecules, the COOH and C–OH appears after the treatment. As shown in Tables 2 and 3, when it has reached a certain time for a longer oxidation reaction, it is easier for the hydroxyl to be transmuted into carboxyl, but the over-handling will cause the C–O/C–OH to combine closely to the PA66 molecules. The carboxyl converts into other substances or just sheds, which results in the fact that few of the carboxyls can be found after being processed for 60 s. We can clearly distinguish the changes of the functional groups varied within the treatment time through the peaks of the corresponding peak-splitting diagrams in Figures 6 and 7. This phenomenon corresponds to the element content changes in Figure 5.

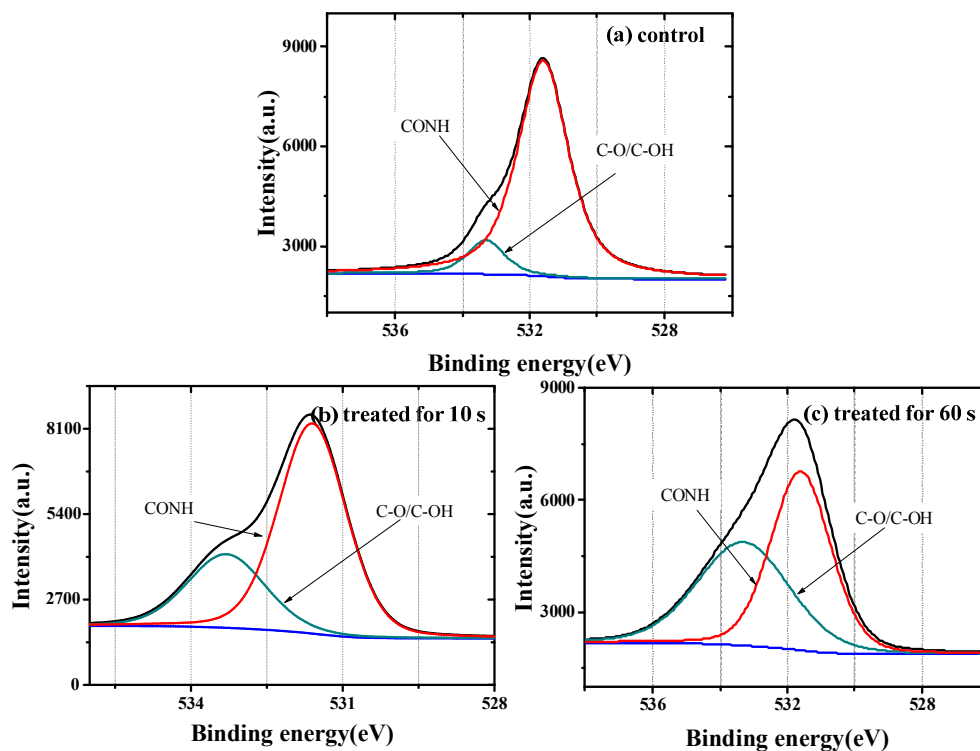


**Figure 7.** Synthesis curve of O1s-spectrums of the control and glow-like plasma processed samples: (a) Control; (b) Treated for 10 s; (c) Treated for 60 s.

### 3.3. Sterilization Effect

The high-energy electrons, ions, other active particles and the ultraviolet rays during the discharge have, to some extent, an inactivation effect on the microorganisms [28]. This kind of inactivation effect is achieved by their damage on the cytomembrane, cytoderm and the genetic material. To study the bactericidal performance of this kind of glow-like plasma, the *Escherichia coli* (*E. coli*) HT115 is chosen to be the test object. Before the experiment, the wire electrodes and the whole reactor are sterilized; the *E. coli* undergoes penicillin resistance processing to eliminate the disturbance from the microbial contamination in the air.

The experimental procedures are as follows: (1) the samples are soaked in 70% alcohol, then placed in the high-pressure steam sterilization pot for drying and sterilizing with the temperature at 121 °C and the pressure is 0.1 MPa; (2) on the clean bench, 10  $\mu$ L bacteria solution (culturing for 13 h) is inoculated onto the PA66 fabric surface and a control group and a series of experimental groups are set; (3) having the samples processed by glow-like plasma under different processing times, the peak voltage is about 90 kV and the PRF is set as 500 Hz. The process is conducted in sterile room; (4) after



the treatment, the region of the PA66 fabric that was inoculated by the *E. coli* is cut off. This piece of fabric is vibrated fully in 5 mL sterile water to elute the thalli. 100  $\mu$ L solution is absorbed and coated onto the solid medium of penicillin resistance; (5) having the solid media of control group and experimental groups cultured in the 37 °C thermostat for a certain time, then the number of *E. coli* colonies are counted on the solid media.

Figure 8 is the effect picture of the atmospheric-air glow-like plasmas processed *E. coli* colonies under different treatment times. Figure 9 gives the changing curve of the number of the *E. coli* colonies with treatment time varied. Figure 8a is the control group, the Figure 8b–h are sterilizing effect pictures of *E. coli* colonies processed 0.5–32 s. During the experiment, the PRF is 500 Hz. It is clear that the sterilizing effect achieved by the glow-like plasma is enhanced with an increase in the treatment time. When the treatment time reaches 32 s, there is nearly no colony appearing on the solid medium. After having 0.5 s of treatment of glow-like plasmas, there is approximately only one-third of the colonies left on the solid medium compared with the control group. These observations prove that this kind of atmospheric-air glow-like plasma has a promising sterilizing effect.

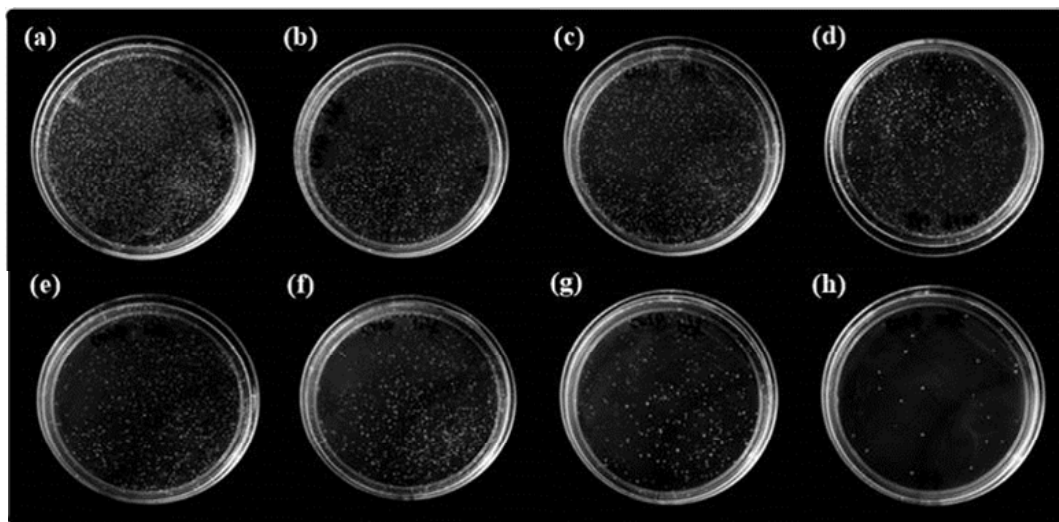


**Figure 8.** Sterilizing effect on *Escherichia coli* achieved by atmospheric air glow-like plasmas: (a) Control; (b) 0.5 s; (c) 1 s; (d) 2 s; (e) 4 s; (f) 8 s; (g) 16 s; (h) 32 s.

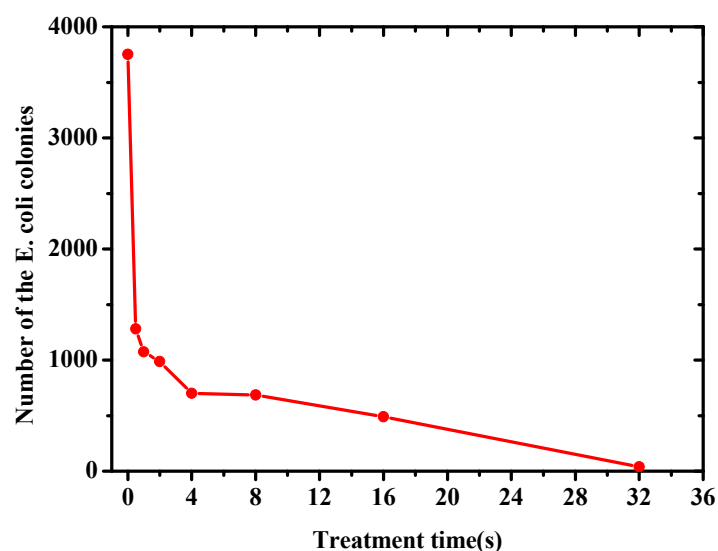


**Figure 9.** Numbers of the *E. coli* colonies with the treatment time varied.

Figure 10 shows the relative numbers of *E. coli* colonies processed by glow-like plasma with PRF varied. The experiment has been repeated three times, the relative deviation is small. It is shown that when the treatment time is constant, the *E. coli* colonies on the solid medium reduce observably along with the increase of the PRF. When PRF increases from 10 to 500 Hz, the number of *E. coli* colonies decreases from 2579 to 87 monotonically. In addition, when the number of discharges is constant, the *E. coli* colonies reduce at first and then increase while the PRF is augmenting. The extreme value point appears at approximately 100 Hz. This is due to the fact that, for a certain treatment time, the higher the PRF, the higher the concentration of the bactericidal-effect active substances in glow-like plasma. It will have a strong impact on the *E. coli* colonies.

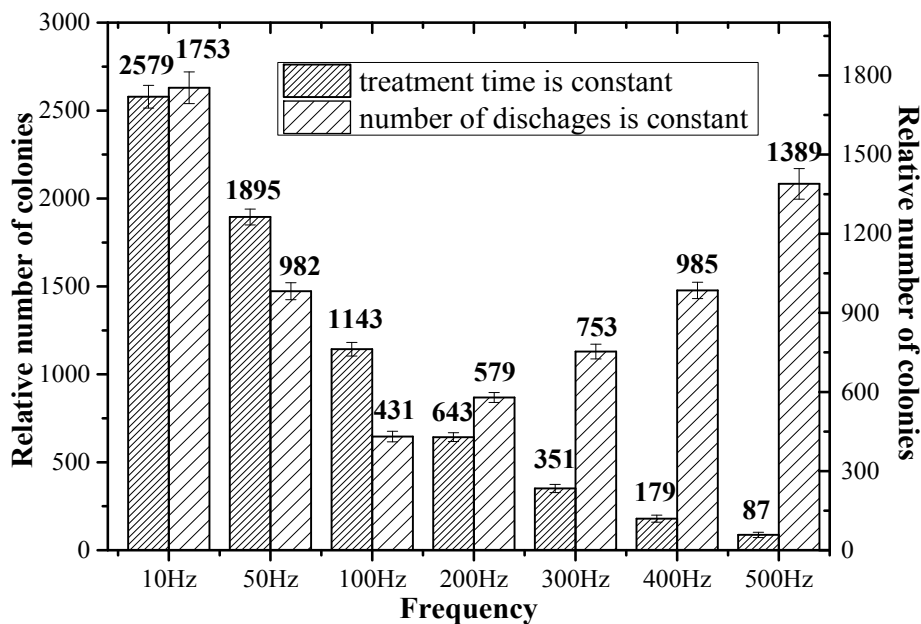
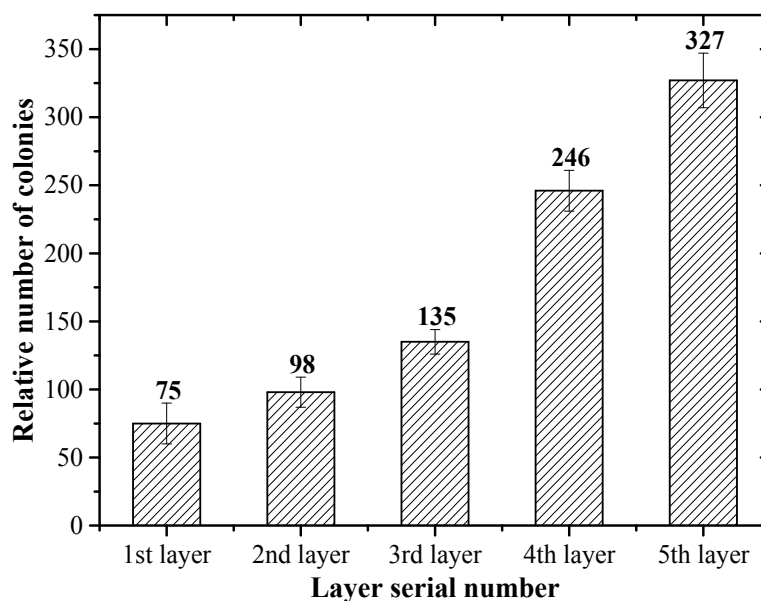


Figure 10. Relative numbers of the *E. coli* colonies with the PRF varied.

With a constant number of discharges, the interval between two sequential pulses is long while the PRF is relatively low. The short-lived active particles in the plasma will disappear, and the long-lived active particles will diffuse to a certain extent, so that the concentration of the bactericidal-effect active substances in the reacting chamber won't be high enough to have a valid sterilizing effect on the *E. coli* on the PA66 fabrics. While the PRF augments to a certain frequency, about 100 Hz, the active particles reach a certain concentration to have the best sterilizing effect on the *E. coli*. However, when the PRF continues augmenting to a certain extent, even though the activity of the plasmas is enhanced, the acting time is too short to have a sufficient contact between the active particles and the PA66 fabrics. As such, the sterilizing effect is weakened. According to this phenomenon in the practical application, the treatment time can be shortened by increasing the PRF. Meanwhile, the same sterilizing effect can be achieved by extending the treatment time at an optimal PRF.

Figure 11 shows the relative numbers of the *E. coli* colonies of the side-by-side processed PA66 fabrics through the atmospheric-air glow-like plasma with when the PRF is 500 Hz. According to the error bar, the relative deviation is small. Before the treatment, the different layers of PA66 fabrics are inoculated by *E. coli* culture solution of the same concentration. During the discharge, the total five layers of PA66 fabrics are placed side-by-side. From the Figure 11, it is shown that the first layer, i.e., the top layer, has the best sterilizing effect with the fewest *E. coli* colonies left; the number is about 75. The bottom layer has the worst sterilizing effect; the number of colonies is about 327. It is still a relatively good treatment effect compared with the Figure 10. The relative number of *E. coli* colonies increases sequentially from the 1st layer to the 5th layer. This is because most of the active particles in

the plasma, which have the bactericidal effect, are absorbed by the top layer—few of them can reach the bottom layer. It should be noted that by extending the treatment time appropriately, the bottom layer can also achieve a better treatment effect. The reasons leading to this phenomenon may be as follows: Firstly, there will be more active particles surrounding the layers of PA66 fabrics while the treatment time increases, and then more active particles can touch the bottom layer. For another, the bactericidal, active substances in the plasma may dissolve in the solution on the fabrics. In that case, some properties, like the acid-base property, may be changed so that the *E. coli* will be inactivated. This solution may penetrate to the bottom layer through the apertures of the PA66 fabrics to influence the corresponding living environment of the *E. coli*.



**Figure 11.** Numbers of the *E. coli* colonies of the side-by-side processed PA66 fabrics.

### 3.4. Aging Effect

Table 4 is focused on the timeliness of this kind of glow-like plasma treatment. In this experiment, five pieces of the PA66 fabrics are processed by the atmospheric-air glow-like plasma with the processing time set at 10 s and the PRF set at 500 Hz. One piece of the processed fabric has been taken out to have the XPS test directly. Two pieces of the processed PA66 fabrics are placed in the air for 1 day and 3 days. The last two pieces of the processed PA66 fabrics are stored in sealed polythene bags for 1 day and 3 days, respectively. They are then tested by XPS. The results of relative chemical compositions and atomic ratios of processed PA66 fabrics stored under different conditions are shown in the Table 4.

**Table 4.** Relative chemical compositions and atomic ratios with storage time and environment varying.

Sample	Element Content (%)			Ratio		
	C1s	O1s	N1s	O/C	N/C	(O + N)/C
Reference	80.11	15.76	4.13	0.20	0.05	0.25
One day (air)	77.08	13.85	9.07	0.18	0.12	0.30
One day (bag)	73.02	17.13	9.85	0.23	0.13	0.36
Three days (air)	77.41	14.17	8.42	0.18	0.11	0.29
Three days (bag)	74.75	16.28	8.96	0.22	0.12	0.34

The plasma treatment can generate oxygen-containing functional groups and it can smooth the surface impurities, which makes the surface energy augmented. That is why plasma treatment is able

to enhance the hydrophilicity of the PA66 samples. However, after the processed samples are laid up under air condition, the impurities will adsorb on the sample once more to reduce the hydrophilicity. So that the aging effect, i.e., the timeliness, is a significant influence factor under industrial application of the surface modification [29]. Comparing the data in the Table 4, laying up the processed samples in the same external conditions, the O/C ratio remains almost unchanged in the air during the storage time. When stored in sealed polythene bags, the O/C ratio of storing for 3 days is only 4.3% less than the one stored for 1 day.

All of the data reveals that this kind of glow-like plasma has relatively good timeliness. Meanwhile, the aging effect can be delayed to some degree. What's more, the sample stored in the sealed polythene bag has the higher O/C ratio while the storage time is constant. This is due to the small quantity of oxygen and impurities that restrict the oxidation-reduction reaction and the repetition pollution, respectively. On the other hand, the less the flow disturbance is, the longer time the newly generated polar functional groups will survive. Tables 5 and 6 give relative amounts of different carbon-containing and oxygen-containing groups with storage time and environment varying.

**Table 5.** Relative amounts of different carbon-containing groups (%) with storage time and environment varying.

Sample	Carbon-Containing Groups (%)			
	C-C	C-N	C-O/C-OH	CONH
One day (air)	42.37	40.20	5.59	11.84
One day (bag)	47.10	27.48	10.19	15.23
Three days (air)	47.74	35.44	5.48	11.35
Three days (bag)	45.60	32.42	9.02	12.96

**Table 6.** Relative amounts of different oxygen-containing groups (%) with storage time and environment varying.

Sample	Oxygen-Containing Groups (%)	
	C-O/C-OH	CONH/COOH
One day (air)	8.73	91.27
One day (bag)	16.53	83.47
Three days (air)	13.25	86.75
Three days (bag)	20.02	79.98

#### 4. Conclusions

This study has obtained large-volume, barrier-free glow-like plasma while a cylindrical electrode configuration is utilized. The treatment is under atmospheric pressure air. The conclusions are as follows:

- (1) Through AFM analyses, the PA66 fabric surface will be etched remarkably by the glow-like plasma. The surface roughness and the surface energy are augmented—all of which may be helpful to ameliorate the PA66 fabric's hydrophilicity.
- (2) The XPS analyses show that after the treatment, the oxygen-containing groups' content rises together with the decrease of the primary C-C and C-N bonds in all, and N-element content has been changed accordingly. This is due to the glow-like plasma cracking the primary carbon-containing bonds, which leads to the formation of hydroxyl, carboxyl and double bonds of carbon to oxygen under atmospheric air at the beginning of the treatment. The COOH and C-OH appears after the treatment. The over-handling will cause the carboxyl to convert into other substances or to shed.
- (3) After almost 30 s of the glow-like plasma treatment for sterilization, most of the *E. coli* inoculated on the PA66 fabrics is inactivated. For the treatment effect of sterilization, when the number of

discharges is constant, the treatment effect doesn't monotonically increase with the augmentation of the PRF. An optimal frequency could be found. When the treatment time isn't the dominant factor, increasing the processing time to a certain degree is beneficial for a better processing effect. Meanwhile, the PRF can be lowered.

- (4) The treatment efficiency obtained by the glow-like plasma can maintain a certain time, i.e., the treatment effect has sufficient timeliness. In addition, the aging effect can be delayed by the sealed storing environment. Before further processing, it is suggested the processed fabrics should be stored in a sealed or oxygen-free environment.

It should be noted that the experimental conclusions can be extended to many kinds of porous polymer fabrics.

**Acknowledgments:** HUST analytical and testing center is gratefully acknowledged for the assistance in AFM and XPS tests. This work is supported by the Fundamental Research Funds for the Central Universities (Grant No. 2016YXZD069) and State Key Laboratory of Advanced Electromagnetic Engineering and Technology, Huazhong University of Science and Technology, Wuhan, China (Grant No. 2017ZZYJ008).

**Author Contributions:** Lee Li proposed the project. Mingyang Peng wrote the main manuscript text. Mingyang Peng, Jiaming Xiong, Kui Hua and Shufan Wang performed the experiments and analyzed the results. Tao Shao advised the technical content and revised the language of the manuscript. All authors reviewed the manuscript.

**Conflicts of Interest:** The authors declare no conflicts of interest.

## References

1. Yousefi, H.R.; Ghoranneviss, M.; Tehrani, A.R.; Khamseh, S. Investigation of glow discharge plasma for surface modification of polypropylene. *Surf. Interface Anal.* **2003**, *35*, 1015–1017. [[CrossRef](#)]
2. Mundo, R.D.; D'Agostino, R.; Palumbo, F. Long-lasting antifog plasma modification of transparent plastics. *ACS Appl. Mater. Interfaces* **2014**, *6*, 17059–17066. [[CrossRef](#)] [[PubMed](#)]
3. Abidi, N.; Hequet, E. Cotton fabric graft copolymerization using microwave plasma. I. Universal attenuated total reflectance–FTIR study. *J. Appl. Polym. Sci.* **2004**, *93*, 145–154. [[CrossRef](#)]
4. Wang, C.X.; Qiu, Y.P. Two sided modification of wool fabrics by atmospheric pressure plasma jet: Influence of processing parameters on plasma penetration. *Surf. Coat. Technol.* **2007**, *201*, 6273–6277. [[CrossRef](#)]
5. Nakahira, A.; Suzuki, Y.; Ueno, S.; Akamizu, H.; Kijima, K.; Nishijima, S. Effect of plasma treatment on microstructure and surface of glass for plastic-based composite. *Sci. Eng. Compos. Mater.* **1999**, *8*, 129–136. [[CrossRef](#)]
6. Shao, T.; Zhou, Y.; Zhang, C.; Yang, W.; Niu, Z.; Ren, C. Surface modification of polymethyl-methacrylate using atmospheric pressure argon plasma jets to improve surface flashover performance in vacuum. *IEEE Trans. Dielectr. Electr. Insul.* **2015**, *22*, 1747–1754. [[CrossRef](#)]
7. Meiners, S.; Salge, J.G.H.; Prinz, E.; Förster, F. Surface modification of polymer materials by transient gas discharges at atmospheric pressure. *Surf. Coat. Technol.* **1998**, *98*, 1121–1127. [[CrossRef](#)]
8. Akishev, Y.; Grushin, M.; Napartovich, A.; Trushkin, N. Novel AC and DC non-thermal plasma sources for cold surface treatment of polymer films and fabrics at atmospheric pressure. *Plasma Polym.* **2002**, *7*, 261–289. [[CrossRef](#)]
9. Akishev, Y.S.; Grushin, M.E.; Monich, A.E.; Napartovich, A.P.; Trushkin, N.I. One-atmosphere argon dielectric-barrier corona discharge as an effective source of cold plasma for the treatment of polymer films and fabrics. *High Energy Chem.* **2003**, *37*, 286–291. [[CrossRef](#)]
10. Lai, J.; Sunderland, B.; Xue, J.; Yan, S.; Zhao, W.; Folkard, M.; Michael, B.D.; Wang, Y. Study on hydrophilicity of polymer surfaces improved by plasma treatment. *Appl. Surf. Sci.* **2006**, *252*, 3375–3379. [[CrossRef](#)]
11. Li, L.; Liu, L.; Liu, Y.L.; Bin, Y.; Ge, Y.F.; Lin, F.C. Analysis and experimental study on formation conditions of large-scale barrier-free diffuse atmospheric pressure air plasmas in repetitive pulse mode. *J. Appl. Phys.* **2014**, *115*, 023301.
12. Teng, Y.; Li, L.; Liu, Y.L.; Liu, L.; Liu, M. Generation of large-scale, barrier-free diffuse plasmas in air at atmospheric pressure using array wire electrodes and nanosecond high-voltage pulses. *Phys. Plasmas* **2014**, *21*, 103510.

13. Zhu, Z.; Zhang, G.; Liu, L.; Li, Y. The research on atmospheric pressure glow-like discharge plasma. In Proceedings of the 33rd IEEE International Conference on Plasma Science, Traverse City, MI, USA, 4–8 June 2006; p. 172.
14. Qi, B.; Ren, C.; Wang, D.; Li, S.Z.; Wang, K.; Zhang, Y. Uniform glowlike plasma source assisted by preionization of spark in ambient air at atmospheric pressure. *Appl. Phys. Lett.* **2006**, *89*, 131503. [[CrossRef](#)]
15. Mei, H.; Feng, J.; Wang, J.; Zhang, X.; Li, Y.; Yan, Y. Synthesis and characterization of nano-HA/PA66 composites. *J. Mater. Sci. Mater. Med.* **2003**, *14*, 655–660.
16. Niu, Z.; Zhang, C.; Shao, T.; Fang, Z.; Yu, Y.; Yan, P. Repetitive nanosecond-pulse dielectric barrier discharge and its application on surface modification of polymers. *Surf. Coat. Technol.* **2013**, *228*, S578–S582. [[CrossRef](#)]
17. Bismarck, A.; Richter, D.; Wuertz, C.; Springer, J. Basic and acidic surface oxides on carbon fiber and their influence on the expected adhesion to polyamide. *Colloids Surf. A Physicochem. Eng. Asp.* **1999**, *159*, 341–350. [[CrossRef](#)]
18. Cai, Z.; Hwang, Y.J.; Park, Y.C.; Zhang, C.; Mccord, M.; Qiu, Y. Preliminary investigation of atmospheric pressure plasma-aided desizing for cotton fabrics. *AATCC Rev.* **2002**, *2*, 18–21.
19. Teng, Y.; Li, L.; Cheng, Y.; Ma, N.; Peng, M.Y.; Liu, M.H. Optical and electrical investigation of a cylindrical diffuse-discharge chamber. *Phys. Plasmas* **2015**, *22*, 033503.
20. Wakida, T.; Lee, M.; Sato, Y. Dyeing properties of oxygen low-temperature plasma-treated wool and nylon 6 fibres with acid and basic dyes. *Color. Technol.* **2008**, *112*, 233–236. [[CrossRef](#)]
21. Yip, J.; Chan, K.; Sin, K.; Kai, L. Study of plasma-etched and laser-irradiated polyamide materials. *Mater. Res. Innov.* **2002**, *6*, 44–50. [[CrossRef](#)]
22. Wavhal, D.S.; Fisher, E.R. Membrane surface modification by plasma-induced polymerization of acrylamide for improved surface properties and reduced protein fouling. *Langmuir* **2002**, *19*, 79–85. [[CrossRef](#)]
23. Fu, R.K.Y.; Mei, Y.F.; Wan, G.J.; Siu, G.G.; Chu, P.K.; Huang, Y.X.; Tian, X.B.; Yang, S.Q.; Chen, J.Y. Surface composition and surface energy of Teflon treated by metal plasma immersion ion implantation. *Surf. Sci.* **2004**, *573*, 426–432. [[CrossRef](#)]
24. Kim, S.H.; Su, H.C.; Lee, N.E.; Kim, H.M.; Yun, W.N.; Kim, Y.H. Adhesion properties of Cu/Cr films on polyimide substrate treated by dielectric barrier discharge plasma. *Surf. Coat. Technol.* **2005**, *193*, 101–106. [[CrossRef](#)]
25. Wha, O.K.; Hun, K.S.; Ae, K.E. Improved surface characteristics and the conductivity of polyaniline–nylon 6 fabrics by plasma treatment. *J. Appl. Polym. Sci.* **2001**, *81*, 684–694.
26. Inagaki, N.; Tasaka, S.; Kawai, H. Surface modification of aromatic polyamide film by oxygen plasma. *J. Polym. Sci. A Polym. Chem.* **2003**, *33*, 2001–2011. [[CrossRef](#)]
27. Inagaki, N.; Tasaka, S.; Kawai, H.; Yamada, Y. Surface modification of aromatic polyamide film by remote oxygen plasma. *J. Appl. Polym. Sci.* **1997**, *64*, 831–840. [[CrossRef](#)]
28. Perni, S.; Shama, G.; Hobman, J.L.; Lund, P.A.; Kershaw, C.J.; Hidalgo-Arroyo, G.A.; Penn, C.W.; Deng, X.T.; Walsh, J.L.; Kong, M.G. Probing bactericidal mechanisms induced by cold atmospheric plasmas with *Escherichia coli* mutants. *Appl. Phys. Lett.* **2007**, *90*, 073902. [[CrossRef](#)]
29. Zille, A.; Fernandes, M.M.; Francesko, A.; Tzanov, T.; Fernandes, M.; Oliveira, F.R.; Almeida, L.; Amorim, T.; Carneiro, N.; Esteves, M.F. Size and aging effects on antimicrobial efficiency of silver nanoparticles coated on polyamide fabrics activated by atmospheric DBD plasma. *ACS Appl. Mater. Interfaces* **2015**, *7*, 13731–13744. [[CrossRef](#)] [[PubMed](#)]

